Design of Electrically Small Wire Antennas Using a Pareto Genetic Algorithm

Hosung Choo, *Member, IEEE*, Robert L. Rogers, *Senior Member, IEEE*, and Hao Ling, *Fellow, IEEE*

***Abstract*—We report on the use of a genetic algorithm (GA) in the design optimization of electrically small wire antennas, taking into account of bandwidth, efficiency and antenna size. For the antenna configuration, we employ a multisegment wire structure. The Numerical Electromagnetics Code (NEC) is used to predict the performance of each wire structure. To efficiently map out this multiobjective problem, we implement a Pareto GA with the concept of divided range optimization. In our GA implementation, each wire shape is encoded into a binary chromosome. A two-point crossover scheme involving three chromosomes and a geometrical filter are implemented to achieve efficient optimization. An optimal set of designs, trading off bandwidth, efficiency, and antenna size, is generated. Several GA designs are built, measured and compared to the simulation. Physical interpretations of the GA-optimized structures are provided and the results are compared against the well-known fundamental limit for small antennas. Further improvements using other geometrical design freedoms are discussed.**

***Index Terms*—Genetic algorithms, small antennas, wire antennas.**

I. Introduction

As THE SIZE OF wireless devices shrinks, the design of electrically small antennas is an area of growing interest [1], [2]. By the classical definition, an electrically small antenna is one that can be enclosed in a volume of radius r much less than a quarter of a wavelength. It is well known that the bandwidth of an electrically small antenna decreases as the third power of the radius [3]–[6]. Much research has been carried out to increase the bandwidth of small antennas using structures such as folded design, disk-loaded monopole, inverted-L or inverted-F designs, multiarmed spiral and conical helix [7]–[10]. Recently, Altshuler reported on the use of a genetic algorithm (GA) in designing electrically small wire antennas [11]. Instead of using a regular shape, he used GA to search for an arbitrary wire configuration in 3-D space that results in maximum bandwidth for a given antenna size.

While much of the small antenna research has been focused on antenna bandwidth, antenna miniaturization also impacts antenna efficiency. The objective of this paper is to apply GA in the design optimization of electrically small wire antennas, taking into account of bandwidth, efficiency and antenna size. To efficiently map out this multiobjective problem, we utilize the Pareto GA [12], [13]. In our implementation, we employ the concept of divided range multiobjective GA [14] to accelerate convergence in the GA process.

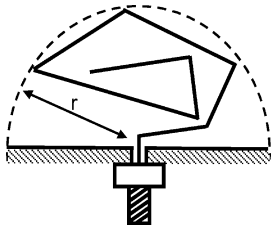

Fig. 1. Configuration of the multisegment wire antenna used in the GA design.

In our approach, we employ the multisegment wire structure similar to the one used in [11]. The Numerical Electromagnetics Code (NEC) [15] is used to predict the performance of each wire structure. We then generate an optimal set of designs by considering bandwidth, efficiency and antenna size. To verify our GA results, several GA designs are built, measured and compared to the simulation. (Some preliminary results were presented earlier in [16].) We also provide physical interpretations of the GA-optimized structures, showing the different operating principles depending on the antenna size. The performance curve achieved by the GA approach is compared against the well-known fundamental limit for small antennas [3]–[6]. To more easily assess the performance of the antennas, we normalize the efficiency-bandwidth product by the antenna size in order to represent the antenna performance as a single figure-of-merit [17]. Finally, we further improve the GA results by exploring other geometrical design freedoms to better approach the fundamental limit.

This paper is organized as follows. In Section II, the details of our GA implementation are described. Section III describes the GA designs and the measurement verification of the results. In Section IV, the GA results are compared to the fundamental limits. In Section V, other design freedoms are explored to further improve performance. Section VI provides conclusions gathered from this research.

II. Pareto GA Approach

The basic antenna configuration considered in this paper is shown in Fig. 1. The antenna is comprised of M connected wire segments. Each segment of the antenna is confined in a hemispheric design space with a radius r and an infinite ground plane. The three design goals are: broad bandwidth, high efficiency

Manuscript received February 10, 2003; revised January 26, 2004. This work was supported in part by the Office of Naval Research under Contract N00014-01-1-0224 and in part by The Texas Higher Education Coordinating Board under the Texas Advanced Technology Program.

H. Choo was with the Department of Electrical and Computer Engineering, The University of Texas at Austin, Austin, TX 78713 USA. He is now with the School of Electronic and Electrical Engineering, Hongik University, Seoul 121-791, Korea (e-mail: hschoo@hongik.ac.kr).

R. L. Rogers is with the Applied Research Laboratories, The University of Texas at Austin, Austin, TX 78713 USA.

H. Ling is with The Department of Electrical and Computer Engineering, The University of Texas at Austin, Austin, TX 78712 USA.

Digital Object Identifier 10.1109/TAP.2004.842404

and small antenna size. We employ the Pareto GA to efficiently map out this multiobjective problem. The advantage of using the Pareto GA over the conventional GA is that a wide range of solutions corresponding to more than one objective can be mapped by running the optimization only once.

In our GA implementation, the hemispheric design space is evenly discretized into 2^n grid points and the location of the each joint of the antenna is encoded into an n-bit binary string. Thus, the total number of bits in the chromosome is nM when we use M connected wire segments. The three costs associated with these design goals are

$$\begin{aligned}\text{Cost } 1 &= 1 - \frac{\text{Antenna Bandwidth}}{\text{Theoretical Bandwidth Limit}}\\ \text{Cost } 2 &= 1 - \text{Efficiency}\\ \text{Cost } 3 &= \text{Antenna Size}(kr).\end{aligned} \tag{1}$$

In the above definition, the theoretical bandwidth limit of $1/((1/kr)+(1/kr)^3)$ derived in [6] is used, where $k = 2\pi/\lambda$ is the wave number. The Numerical Electromagnetics Code (NEC) [15] is used to predict the antenna performance in order to compute the cost functions. Multiple Linux machines are used in parallel to carry out this computation.

After evaluating the three cost functions of each sample structure using NEC, all the samples of the population are ranked using the nondominated sorting method [18]. Here, the higher the rank (1 denotes the highest rank), the better the solution. This method assigns rank-1 to the nondominated solutions of the population. The term nondominated solution means that there are no other solutions that are superior to this solution with respect to all design objectives. Then the next nondominated solutions among the remaining solutions are assigned rank-2. The process is iterated until all the solutions in the population are ranked. Based on the rank, a reproduction process is performed to refine the population into the next generation. The set of rank-1 solutions is termed the Pareto front. By favoring the higher-ranked solutions in the reproduction process, the Pareto GA tries to push the Pareto front as close to the optimum solution in the cost space as possible. Note that since we are only interested in designs with a nonzero -3 dB bandwidth, we prohibit those designs with zero bandwidth from entering the rank one group.

For the crossover operation, a two-point crossover scheme involving three chromosomes is used. The process selects three chromosomes as parents and divides each chromosome into three parts. The three parent chromosomes are then intermingled by taking one part from each of the three parent chromosomes to create three child chromosomes. For numerical stability, a geometrical check is applied to prevent the wires from intersecting one another. In order to avoid the solutions

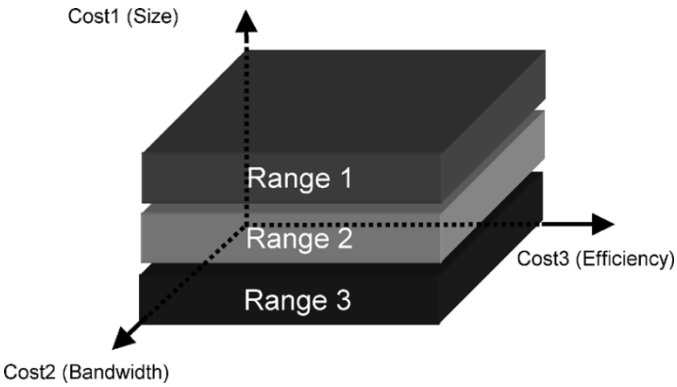

Fig. 2. Divided range multiobjective GA approach.

from converging to a single point, we perform a sharing scheme described in [19] to generate a well-dispersed population. In the sharing process, the rank is modified by penalizing those members on the front that are too close to each other in the cost space. This is accomplished by multiplying a niche count (m_i) to the assigned rank. The niche count is calculated according to

$$m_i = \frac{1}{N_p}\sum_{j=1}^{N_p} Sh\,(d_{ij}) \tag{2}$$

where the N_p is the number of rank-1 members and the sharing function, $Sh(d_{ij})$, is a function of the cost distance between solutions expressed in (3) at the bottom of the page. As we can see, the sharing function increases linearly if other members on the front are closer than d_{share} from a chosen member i in the cost space. Consequently, those members that have close-by neighbors in the cost space are assigned lower ranks in the reproduction process.

We found that the standard Pareto GA did not always give satisfactory results in this problem since it is much harder for small-sized antennas to achieve a nonzero -3 dB bandwidth than for large-sized antennas. Thus, large-sized antennas usually dominate the whole population after several generations of the GA process. As a result, the final Pareto front contains only antenna designs with sizes greater than $kr = 0.45$. To avoid this bias, we employ the concept of the divided range multiobjective GA [14] in our implementation. As shown in Fig. 2, we partition the size into multiple ranges and carry out the Pareto GA on each range individually. After each range converges to an optimal solution, we merge the populations from all ranges and optimize the combined population in the last step of this process. This algorithm shows much improved performance for this more difficult multiobjective problem. Using the scheme we can achieve good results for small-sized antennas ($kr < 0.45$) as well as large-sized ones ($kr > 0.45$).

$$Sh(d_{ij}) = \begin{cases} 2 - \frac{d_{ij}}{d_{\text{share}}} & \text{if } d_{ij} < d_{\text{share}} \\ 1 & \text{if } d_{ij} > d_{\text{share}} \end{cases}$$
$$d_{ij} = \sqrt{(\text{Cost1}(i) - \text{Cost1}(j))^2 + (\text{Cost2}(i) - \text{Cost2}(j))^2 + (\text{Cost3}(i) - \text{Cost3}(j))^2}. \tag{3}$$

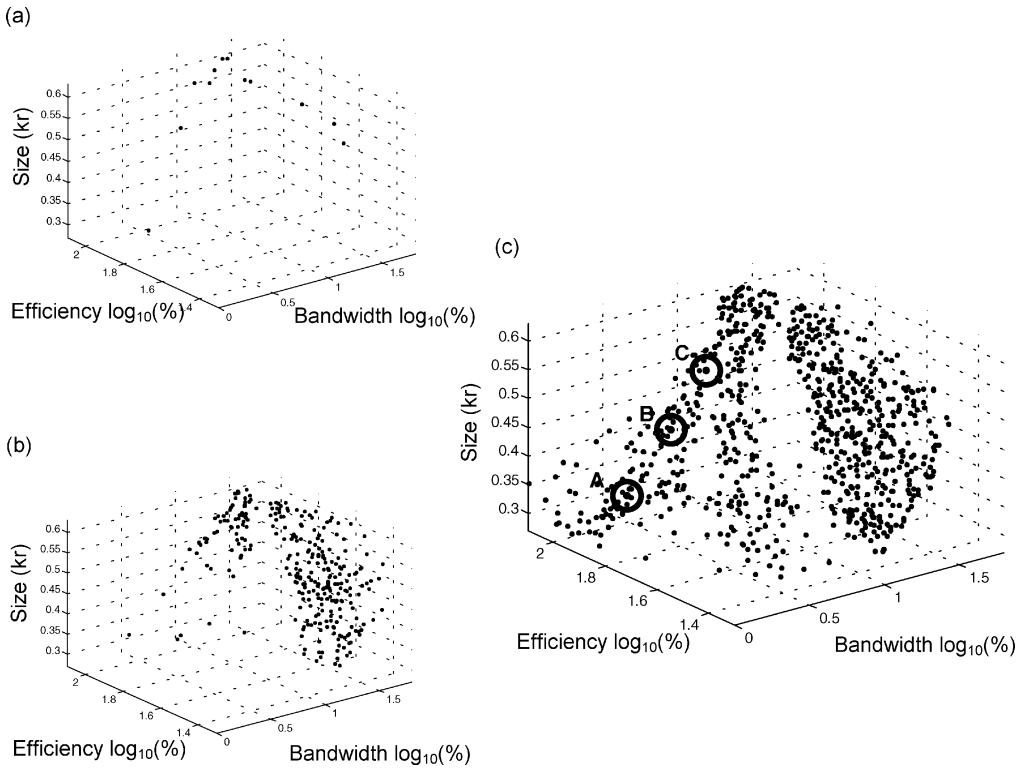

Fig. 3. Convergence of the Pareto front as a function of the number of generations for bandwidth, efficiency and antenna size. (a) Initial generation. (b) After 200 generations. (c) After 1000 generations.

III. GA-Optimized Results

A. GA Optimized Designs

In this section, we investigate the optimal antenna shapes that give rise to the best efficiency-bandwidth (EB) product for a given antenna size. Seven wire segments are used in the antenna configuration. The wire radius is chosen to be 0.5 mm. The antenna is assumed to be fed from the center of the hemisphere. We discretize the 3-D hemisphere with radius r into 2^{15} points and the locations of the 7 wire segments are encoded as a binary chromosome of 7×15 bits. In addition, we add an extra three bits for choosing 7 different wire conductivities including 5.7×10^7 S/m (copper), 3.8×10^7 (aluminum), 1.0×10^7 (iron), 7.0×10^6 (lead), 1.1×10^6 (stainless steel), 6.3×10^5 (NdFe30) and 7×10^4 (graphite). The population size is chosen to be 2000 and we divide the population into four sub ranges ($0.29 \leq kr < 0.38$, $0.38 \leq kr < 0.46$, $0.46 \leq kr < 0.54$ and $0.54 \leq kr < 0.63$). Each range has a population size of 500. A crossover probability of 0.8, a mutation probability of 0.1 and a d_{share} distance of 1 are used. The target design frequency is chosen at 400 MHz and an infinite ground plane is assumed in the simulation. All antennas are designed to match to a 50 Ω impedance. The total computational time is about 20 hours using four Pentium IV 1.7 GHz machines running in parallel. Fig. 3(a)–(c) show the designs in the population with a rank of 1 at, respectively, the initial, 200 and 1000 generations of the Pareto GA process. The three axes are the bandwidth, efficiency and antenna size. Each dot represents a particular rank-1 design. We can see that in the initial generation, only a few rank-1 solutions exist. After 200 generations, many more rank-1 solutions appear. After 1000 generations, a large portion of solutions (770 over 2000) is on the Pareto front. The solutions are relatively well spread out over the Pareto front due to the sharing operation.

B. Verification of the GA-Optimized Results

To verify our GA results, three GA-optimized designs are selected from the Pareto front [at points A ($kr = 0.34$), B ($kr = 0.42$) and C ($kr = 0.5$)] and are shown in Fig. 4. The smallest sample, at point A, somewhat resembles a helix, while the largest sample C resembles a complicated loop where the end of the wire is connected to the ground plane. The total lengths of the wire for the three designs are 28.2, 30.5, and 53.1 cm for designs A, B, and C, respectively. The three designs were built and their performances were measured. We used copper wire of radius 0.5 mm, and a 1.6 m $\times$ 1.6 m conducting plate as the ground plane. Fig. 5(a) is a photo of design B and Fig. 5(b) is the resulting return loss (decibels) as a function of frequency by simulation and measurement. Except for a slight (3%) shift in the resonant frequency, the simulation and measurement results show nearly the same bandwidth (about 5.3% based on $|S_{11}| \leq -3$ dB). Fig. 5(c) is the resulting efficiency of the antenna. We used the standard Wheeler cap method [20], [21] to measure the efficiency. The measured efficiency matches the simulation well at the resonant frequency of 400 MHz, as indicated by the arrow in Fig. 5(c). At other frequencies, the agreement is also good except in the neighborhood of 385 MHz. The

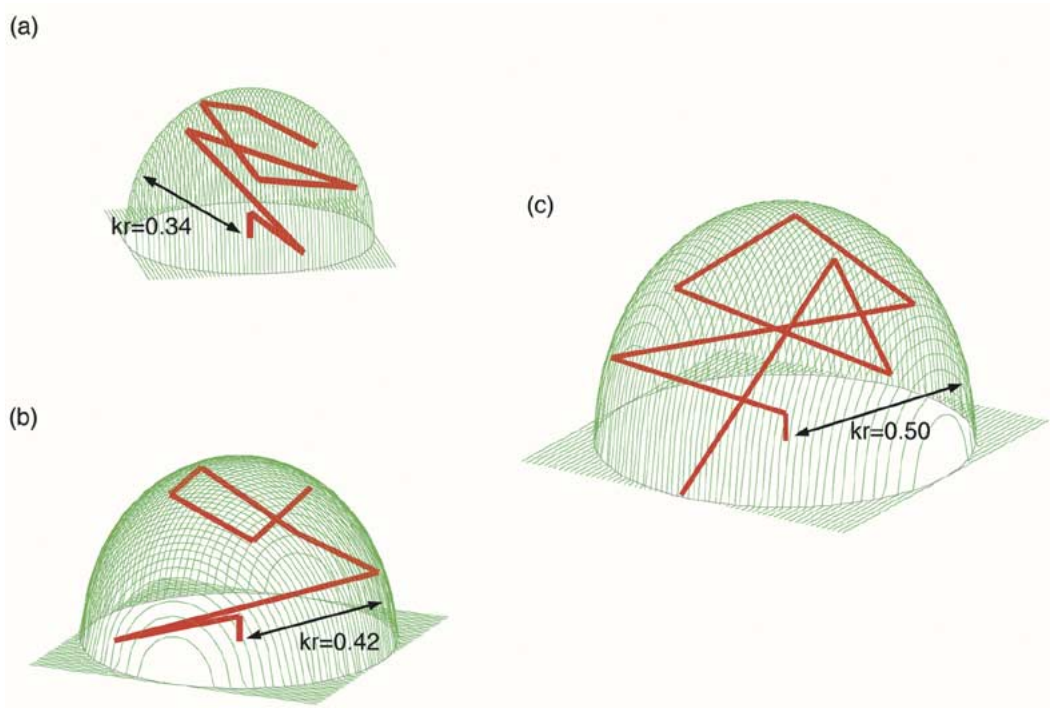

Fig. 4. Three samples from the Pareto front. (a) $kr = 0.34$. (b) $kr = 0.42$ (c) $kr = 0.50$.

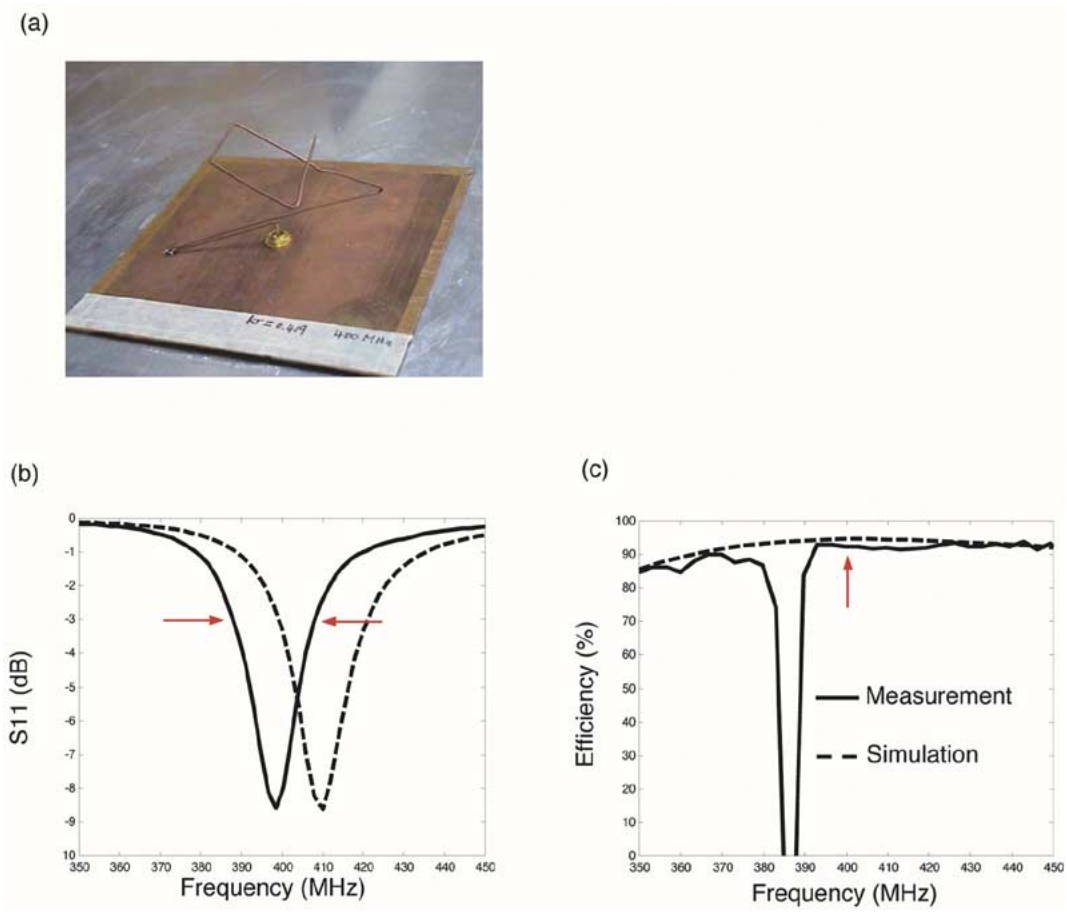

Fig. 5. (a) Photo for antenna B, which has a size of $kr = 0.42$. (b) Return loss and (c) efficiency versus frequency of antenna B. The efficiency measurement was done using the Wheeler cap method.

presence of the large efficiency dip based on the measured data is due to an anti-resonance in the antenna, as the Wheeler cap method fails near this anti-resonance. Similar good agreements were also found for antennas A ($kr = 0.34$) and C ($kr = 0.50$).

TABLE I
RESONANT FREQUENCY, VSWR, BANDWIDTH, AND EFFICIENCY FOR THE SAMPLE ANTENNAS A, B, AND C BY SIMULATION AND MEASUREMENT

	Resonant Freq f_c (MHz)		VSWR at f_c		Bandwidth (-3dB)		Efficiency (%)	
	Simulated	Measured	Simulated	Measured	Simulated	Measured	Simulated	Measured
Ant. A	404	394	1.28	1.96	2.5 %	2.1 %	88 %	84 %
Ant. B	414	407	2.18	2.18	5.5 %	5.3 %	94 %	92 %
Ant. C	411	401	2.80	2.72	9.8 %	8.5 %	97 %	94 %

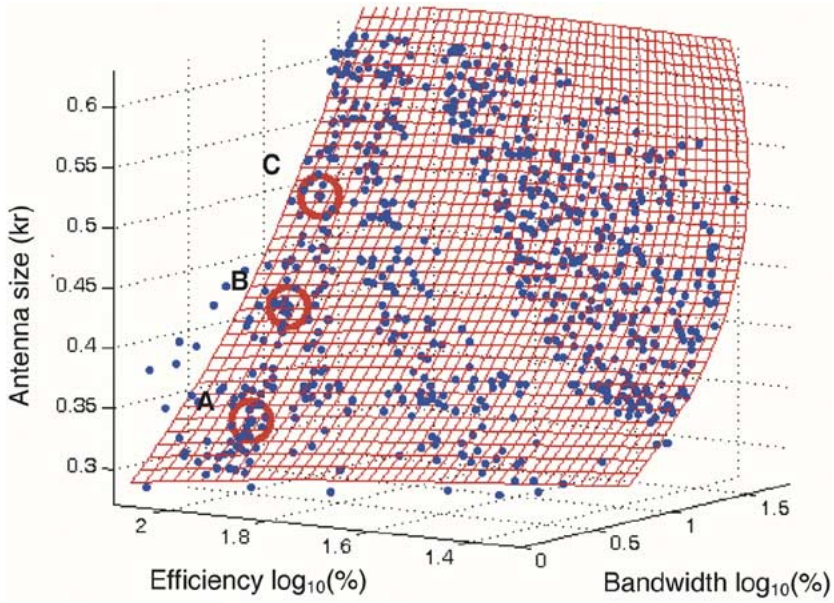

Fig. 6. Pareto front of the GA designs after convergence. The surface is generated using a least squares fitting to best fit the GA results shown as dots.

The results are summarized in Table I. We note that both the achievable bandwidth and efficiency drop as the antenna size is reduced.

C. Physical Interpretation of GA-Optimized Design

By examining the GA-optimized antenna structure in Fig. 4(c), we see that the end of the antenna is connected to the ground plane. Closer examination reveals that a large portion of the antennas with $0.45 < kr < 0.65$ on the Pareto front have this characteristic, which is similar to a folded monopole antenna. Since a folded monopole has four times the input impedance of a standard monopole [22], the GA-designed antennas use this basic structure to boost up the impedance of the antenna to approach 50 Ω. For antenna designs of this type, the total electrical length of the wire ranges between 0.5λ and 0.8λ. The remaining portion (about 30%) of the optimal designs in the $0.45 < kr < 0.65$ range appear to resemble top-loaded structures, with wire segments clustered near the top of the antennas. The total electrical length of the wire for this type of design ranges between 0.3λ and 0.5λ.

As we examine at the GA-optimized structures for even smaller-sized antennas ($kr < 0.45$) such as those in Fig. 4(a) and (b), we find that the electrical lengths are in the 0.3λ and 0.5λ range. More interestingly, most of the antennas are shorted to the ground plane at the joint between the first and second segments from the feed. This turns the first segment into an inductive feed. Segments 2 through 7 become the radiating part of the antenna, carrying most of the current. The strength of the inductive coupling depends on the distance between the first and second segments. Since inductive coupling can greatly increase the input impedance, the GA finds this as an optimized structure for very small-sized antennas ($kr < 0.45$), which need a large impedance step-up to get to 50 Ω. We have investigated this concept in more detail in order to design very small antennas and the results are reported in [23].

IV. COMPARISON TO FUNDAMENTAL LIMIT

In this section, our GA results are compared to the fundamental limits for small antennas. Fig. 6 depicts all of the GA-optimized designs on the Pareto front plotted in the 3-D bandwidth,

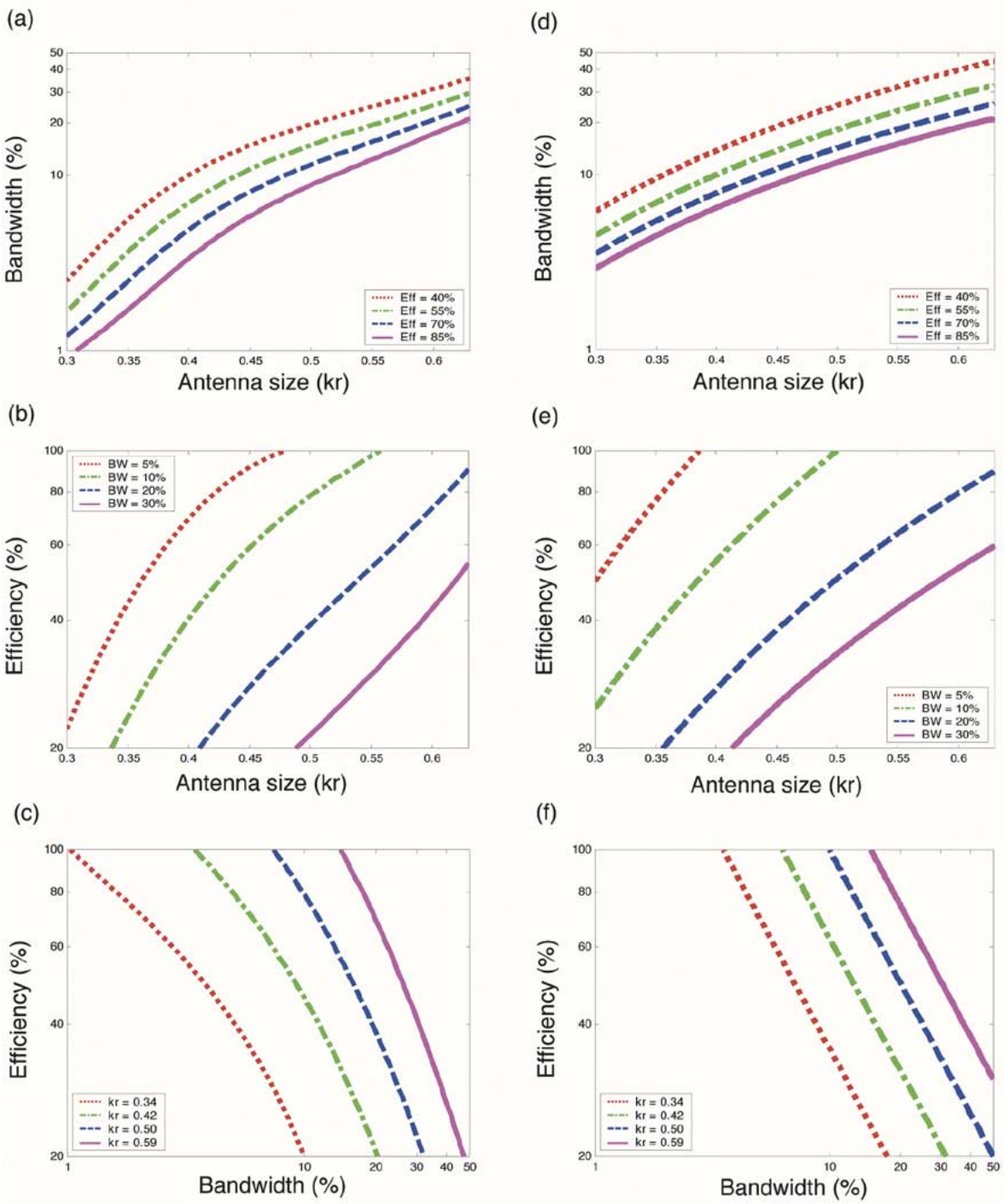

Fig. 7. (a) Projection of the Pareto front to the size and efficiency plane. (b) Projection of the Pareto front to the size and bandwidth plane. (c) Projection of the Pareto front to the bandwidth and efficiency plane. (d)–(f) Corresponding fundamental limit based on (4).

efficiency and antenna size space. We used a least squares fit to create a surface that best fits our GA results. To more easily interpret the results, we project the 3-D plot onto three planes, and the results are shown in Fig. 7(a)–(c). Then, we compare these GA results to the well-known fundamental limit using a combination of equations in [5] and [6]

$$\mathrm{BW} = \frac{1}{\mathrm{Eff} \times Q} \qquad \text{where } Q = \frac{1}{kr} + \frac{1}{(kr)^3}. \tag{4}$$

The curves based on (4) are shown in Fig. 7(d)–(f). Fig. 7(a) shows the maximum bandwidth curve achievable by the GA designs as a function of antenna size for different efficiencies. As expected, for a given efficiency, the achievable bandwidth decreases as the antenna size is reduced. Also, the higher the efficiency, the lower the achievable bandwidth. It is similar to the trend of the fundamental limit in Fig. 7(d). However, our GA performance is lower than the fundamental limit. Fig. 7(b) is the projection of GA designs on the antenna size vs. efficiency plane. For a given bandwidth, the achievable efficiency decreases as the antenna size is reduced. This trend can also be

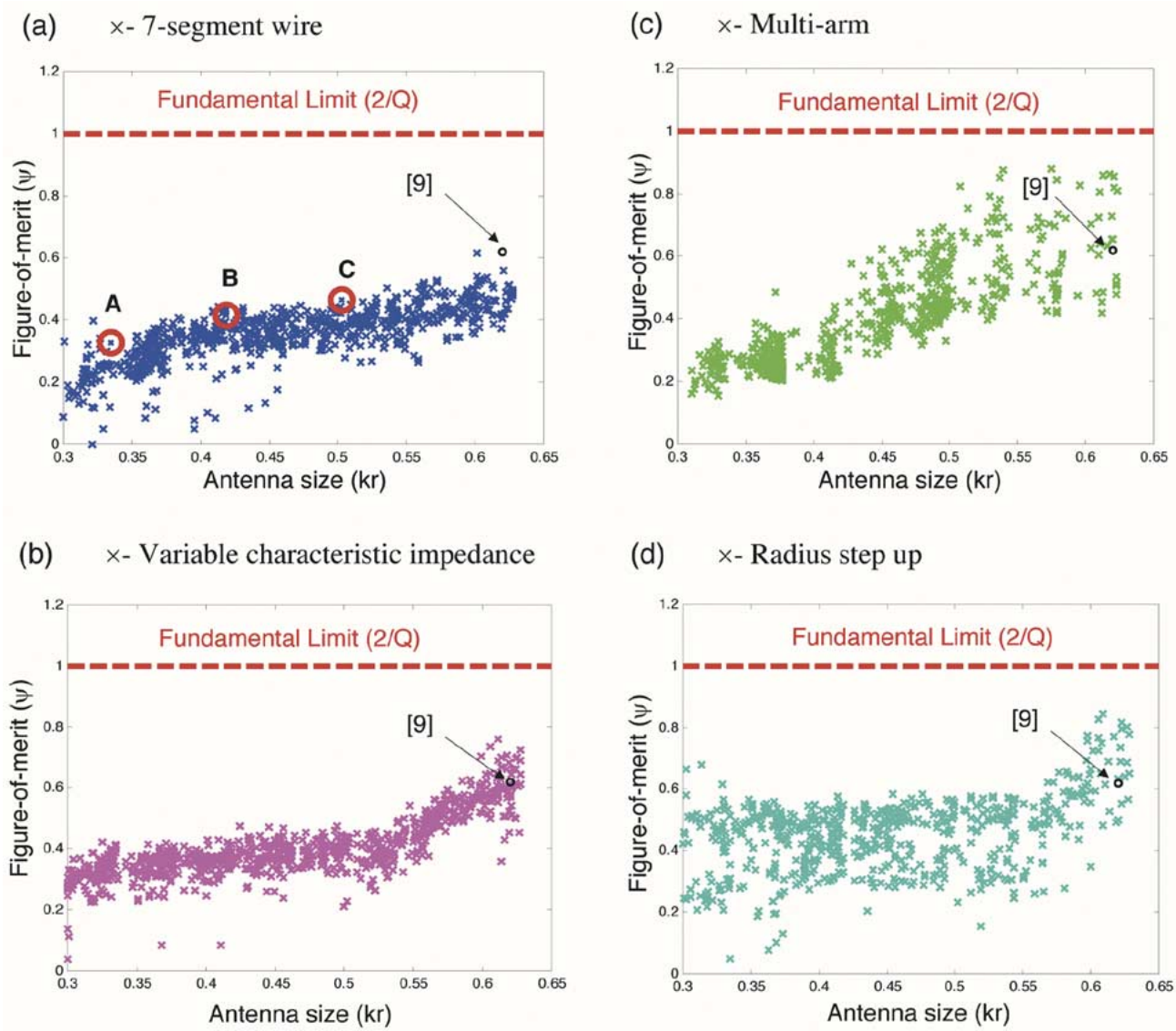

Fig. 8. Small antenna performance using the definition of $\psi = \text{Eff} \times \text{BW}/(\text{Theoretical BW Limit})$. (a) Original 7-wire configuration. (b) Variable input impedance. (c) Multi-arm configuration. (d) Multiple wire radii.

observed in Fig. 7(e). Fig. 7(c) is the projection of the GA results on the bandwidth vs. efficiency plane. For a given antenna size, the tradeoff between antenna bandwidth and antenna efficiency can be clearly seen. Again, the trend on this graph is similar to the fundamental limit in Fig. 7(f).

To make the antenna performance easier to assess, we use the figure-of-merit ψ suggested in [17]

$$\psi = \frac{\text{Eff} \times \text{BW}}{\frac{2}{Q}} \tag{5}$$

where Q is given in (4) and an extra factor of 2 is used to account for the loaded Q. Using this expression, the fundamental limit on ψ is always 1 for antennas of arbitrary sizes. All of the GA-optimized designs are re-plotted using this figure-of-merit in Fig. 8(a). As a reference, we plot the disk-loaded monopole from [9] on the same figure. As we can see, most of the GA designs are below $\psi = 0.5$. The smaller the antennas, the worse the performance of the GA designs. Next we investigate ways to further improve the GA designs.

V. Further Improvement on GA Designs

To bring the figure-of-merit of our designs even closer to the fundamental limit, we explore additional design freedoms to our original 7-wire configuration. First, we increase the number of segments up to 16 wires. However, the results show almost no improvement compared to the original 7-wire ones. Next, we permit the selection of characteristic impedance to vary between 1 Ω to 300 Ω, instead of requiring a fixed 50 Ω for the input port. This is the assumption used in the work of Altshuler [11], who assumes that a perfect impedance transformer is available. When allowed this freedom, our GA produced the results plotted in Fig. 8(b). As the graph shows, using variable characteristic impedance only gives a slight improvement in performance over the original design plotted in Fig. 8(a).

We then examine how a multiarm configuration can improve antenna performance. We use two arms for the antennas structure and the resulting figure-of-merits are shown in Fig. 8(c). It shows good improvement for large-sized antennas ($kr >$

0.45). Using the multiarm configuration, the antenna efficiency is increased while the antenna bandwidth is preserved. This is achieved by spreading the current on multiple branches and lowering the power dissipation. However, the multiarm design does not show much improvement for small-sized antennas ($kr < 0.45$). We further increase the number of arms to 4, but adding more number of arms does not show more improvement over the two-arm design. We believe it is due to the difficulty in packing a multiarm structure in a limited design space.

Finally, we try to increase the degree of freedom by allowing for two different wire radii in each design. The resulting antenna has one wire radius for the lower portion of the antenna and another for the upper portion. Stepping the wire radius has the effect of increasing the input impedance, similar to the way a radius step up is used in a folded monopole design. Since it is known that the NEC version 2 we use in the simulation does not accurately model the wire radius change, we limit the radius change to less than 2. Fig. 8(d) shows the result of the design. It shows improved performance for both small-sized antennas and large-sized antennas. Based on these preliminary results, it appears that the use of targeted design freedoms can further improve the performance of the GA-optimized designs toward the fundamental limit.

VI. Conclusion

The Pareto GA has been applied to design electrically small wire antennas by considering antenna bandwidth, efficiency and size. Wire structures comprising of multiple segments were considered. While the qualitative tradeoffs among the three objectives are well known, this problem is unique in that the theoretical limits exist, and a fundamental issue is how close practical designs can quantitatively approach the theoretical limits. Pareto GA offers an approach to map out the optimal designs in this multiobjective problem very efficiently. A whole series of optimal designs of varying size, bandwidth and efficiency can be generated efficiently in a single GA run. By incorporating the concept of the divided range GA, we achieved a well-formed Pareto front in terms of the three objectives. To verify our GA results, we built several antennas based on the GA designs and measured their bandwidth and efficiency. Both the bandwidth and efficiency measurements agreed well with the simulation for all the sample antennas.

The performance achieved by the GA designs was also compared against the well-known fundamental limit for small antennas. Our resulting GA designs followed the trend of the fundamental limit, but were about a factor of two below the limit. To further improve the performance of the GA-designed antennas, we explored other design freedoms such as variable characteristic impedance, multiarm wires and multiple wire radii. Results showed that the use of targeted design freedoms could further improve the optimization performance toward the fundamental limit.

References

[1] A. K. Skrivervik, J. F. Zurcher, O. Staub, and J. R. Mosig, "PCS antenna design: The challenge of miniaturization," *IEEE Antennas Propag. Mag.*, vol. 43, pp. 12–27, Aug. 2001.

[2] J. P. Gianvittorio and Y. Rahmat-Samii, "Fractal antennas: A novel antenna miniaturization technique, and applications," *IEEE Antennas Propag. Mag.*, vol. 44, pp. 20–36, Feb. 2002.

[3] H. A. Wheeler, "Fundamental limitations of small antennas," *Proc. IRE*, vol. 35, pp. 1479–1484, Dec. 1947.

[4] L. J. Chu, "Physical limitations of omni-directional antennas," *J. Appl. Phys.*, vol. 19, pp. 1163–1175, Dec. 1948.

[5] R. C. Hansen, "Fundamental limitations in antennas," *IEEE Antennas Propag. Mag.*, vol. 69, pp. 170–182, Feb. 1981.

[6] J. S. McLean, "A re-examination of the fundamental limits on the radiation Q of electrically small antennas," *IEEE Trans. Antennas Propag.*, vol. 44, no. 5, pp. 672–676, May 1996.

[7] R. C. Johnson, *Antenna Engineering Handbook*. New York: McGraw-Hill, 1993.

[8] C. H. Friedman, "Wide-band matching of a small disk-loaded monopoles," *IEEE Trans. Antennas Propag.*, vol. 33, no. 10, pp. 1142–1148, Oct. 1985.

[9] H. D. Foltz, J. S. McLean, and G. Crook, "Disk-loaded monopoles with parallel strip elements," *IEEE Trans. Antennas Propag.*, vol. 46, no. 12, pp. 1894–1896, Dec. 1998.

[10] J. A. Dobbins and R. L. Rogers, "Folded conical helix antenna," *IEEE Trans. Antennas Propag.*, vol. 49, pp. 1777–1781, Dec. 2001.

[11] E. E. Altshuler, "Electrically small self-resonant wire antennas optimized using a genetic algorithm," *IEEE Trans. Antennas Propag.*, vol. 50, no. 3, pp. 297–300, Mar. 2002.

[12] D. Goldberg, *Genetic Algorithms in Search, Optimization and Machine Learning*. Reading, MA: Addison Wesley, 1989.

[13] Y. Rahmat-Samii and E. Michielssen, *Electromagnetic Optimization by Genetic Algorithms*. New York: Wiley, 1999.

[14] T. Hiroyasu, M. Miki, and S. Watanabe, "The new model of parallel genetic algorithm in multi-objective optimization problems – Divided range multi-objective genetic algorithm," in *Proc. Congress Evolutionary Computation*, vol. 1, 2000, pp. 333–340.

[15] G. J. Burke and A. J. Poggio, *Numerical Electromagnetics Code (NEC)-Method of Moments*, CA: Lawrence Livermore Laboratory, 1981.

[16] H. Choo, H. Ling, and R. L. Rogers, "Design of electrically small wire antenna using genetic algorithm taking into consideration of both bandwidth and efficiency," in *Proc. IEEE Antennas and Propagation Soc. Int. Symp.*, vol. 1, San Antonio, TX, Jun. 2002, pp. 330–333.

[17] R. L. Rogers, D. P. Buhl, H. Choo, and H. Ling, "Size reduction of a folded conical helix antenna," in *IEEE Antennas and Propagation Soci. Int. Symp.*, San Antonio, TX, June 2002, pp. 34–37.

[18] N. Srinivas and K. Deb, "Multiobjective optimization using nondominated sorting in genetic algorithm," *J. Evolutionary Computation*, vol. 2, pp. 221–248, 1995.

[19] J. Horn, N. Nafpliotis, and D. E. Goldberg, "A niched Pareto genetic algorithm for multiobjective optimization," in *Proc. 1st IEEE Conf. Evolutionary Computation*, vol. 1, 1994, pp. 82–87.

[20] H. A. Wheeler, "The radiansphere around a small antenna," *Proc. IRE*, vol. 47, pp. 1325–1331, Aug. 1959.

[21] E. H. Newman, P. Bohley, and C. H. Walter, "Two methods for the measurement of antenna efficiency," *IEEE Trans. Antennas Propag.*, vol. 23, no. 4, pp. 457–461, Jul. 1975.

[22] C. A. Balanis, *Antenna Theory Analysis and Design*. New York: Wiley, 1997.

[23] H. Choo and H. Ling, "Design of electrically small planar antennas using inductively coupled feed," *Elect. Lett.*, vol. 39, pp. 1563–1564, Oct. 2003.

Hosung Choo (S'00–M'04) was born in Seoul, Korea, in 1972. He received the B.S. degree in radio science and engineering from Hanyang University in Seoul, Korea, in 1998, and the M.S. and Ph.D. degrees in electrical and computer engineering from the University of Texas at Austin, in 2000 and 2003, respectively.

From 1999 to 2003, he was a Research Assistant with the Department of Electrical and Computer Engineering, University of Texas at Austin. In September 2003, he joined the School of Electronic and Electrical Engineering, Hongik University, Seoul, Korea, where he is currently a Full-time Instructor. His principal area of research is the use of the genetic algorithm in developing microstrip and wire antennas and microwave absorbers. His studies include broadband and multiband antennas for wireless communications and miniaturized antennas for RFID applications.

Robert L. Rogers (M'98–SM'99) was born in San Angelo, TX, in 1961. He received the B.S., M.S.E., and Ph.D. degrees from The University of Texas at Austin, in 1983, 1985, and 1989, respectively, all in electrical engineering.

Upon graduation, he joined the Applied Research Laboratories, The University of Texas at Austin, where he is currently a Principal Investigator. He has been involved in the areas of microwave and millimeter-wave antennas, electrically small antennas, radar, radiometry, communications systems, and high-power pulsed energy systems. His research interests are in the areas of remote sensing, communications, wireless networking, and antennas.

Hao Ling (S'83–M'86–SM'92–F'99) was born in Taichung, Taiwan, on September 26, 1959. He received the B.S. degrees in electrical engineering and physics from the Massachusetts Institute of Technology, Cambridge, in 1982, and the M.S. and Ph.D. degrees in electrical engineering from the University of Illinois at Urbana-Champaign, in 1983 and 1986, respectively.

During 1982, he was associated with the IBM Thomas J. Watson Research Center, Yorktown Heights, NY, where he conducted low temperature experiments in the Josephson Department. He joined the faculty of the University of Texas at Austin in September 1986 and is currently Professor of Electrical and Computer Engineering and holder of the L. B. Meaders Professorship in Engineering. He participated in the Summer Visiting Faculty Program in 1987 at the Lawrence Livermore National Laboratory. In 1990, he was an Air Force Summer Fellow at Rome Air Development Center, Hanscom Air Force Base. His principal area of research is in computational electromagnetics. During the past decade, he has actively contributed to the development and validation of numerical and asymptotic methods for characterizing the radar cross section from complex targets. His recent research interests also include radar signal processing, automatic target identification, antenna design and physical layer modeling for wireless communications.

Dr. Ling was a recipient of the National Science Foundation Presidential Young Investigator Award in 1987, the NASA Certificate of Appreciation in 1991, as well as several teaching awards from the University of Texas.